

# Analytical Approach of Sliding Installation Method with Spar Structure

† Jong-Hyun Lee

† Offshore Wind Power Research Project Team, RIST, Incheon 406-840, Republic of Korea

**Abstract :** It is important to understand the trajectory of structure in launching process because of the short time of launching process may result in unexpected accidents or damage to structures. The high risk of structural failure is not avoidable without the fully comprehension of changing forces in launching procedure. The commercial software can evaluate the motion of launching event in calm water condition but there is the limitation of research application because of the programmed commercial software. The launching process of the spar hull is suggested with stage concept that is divided into 10 stages in time domain. A force equilibrium diagram is derived for each stage where the changes of force vector and motion characteristics take place. In particular, the effects of changes in buoyancy and drag force due to the progressive submergence of the spar hull are taken into account by means of a touch length concept. The results contained in this paper provide the valuable information of the trajectory motion evaluation with suggested methods in spar launching process with sliding barge. Furthermore, the presented stage concept and touch length concept will provide basic knowledge for understanding launching process and help to develop further research area for launching analysis.

**Key words :** Equilibrium diagram, Offshore launching, Spar, Sliding barge, Sliding installation method

## 1. Introduction

The launching operation is the most critical part of the entire installation procedure. The failure of launching could result in damage to local members, damage to the transportation barge, overturning of the units (spar and barge together), and even total loss of the structure. Whatever the cause, the failure of the launching makes the delay of the project and the economic loss (Noble Denton and Associates Inc. 1984).

There are several reasons for selecting the sliding type of launching. Firstly, the spar hull structure is too heavy to be lifted. Secondly, the transport barge not only carries the spar hull in a relatively short time than a wet tow type but also can launch it without using a crane vessel. Local loads and relative movements rather than global loading are critical during the sliding launching operations. The updated technical development can evaluate the launching procedure with calm water condition in time domain, but it is not developed yet for the wave considered case. There is limitation of application of real environmental conditions because of the assumption of calm water so the wave considered launching analysis is needed.

The suggested method of a launching analysis is based on a time history of the two component bodies with equilibrium conditions. Launch simulations are divided into several stages

through specific defined times and conditions. Each stage has a dynamic loading analysis, a motion analysis and a trajectory calculation. Stability and dynamic loadings in the intermediate stages are also examined. The analytical approach of launching a spar hull into the sea from a transport barge is carried out to establish the physical model of launching process for the application of sea conditions.

## 2. Governing equation of launching motion

The launching simulation is divided into several stages namely from Stage 1 to 10, with equilibrium conditions governed by external circumstances. A local coordinate system, o-xyz, fixed to the barge is used to examine the motion of the spar relative to the barge. A space-fixed global coordinate system, O-XYZ, is used to calculate the barge movements which are mainly caused by the reactive acceleration force due to the inertia of the spar hull.

The governing equations of the barge in surge, heave and pitch modes of motion are written as:

$$\sum_{k=1,3,5} \left[ \left( m_{jk}^S(t) + m_{jk}^B(t) + A_{jk}^{B(\infty)} \right) \ddot{\xi}_{jk}^B + \left[ B_{jk}^B(t) \dot{\xi}_{jk}^B + C_{jk}^B(t) \xi_{jk}^B = F_j^W(t) + F_j^E(t) \right] \right] \quad (1)$$

where the superscripts S and B are stand for the spar and barge respectively.  $B_{jk}$  and  $C_{jk}(t)$  are damping and restoring

† Corresponding author, naoe@rist.re.kr 032) 200-2486

Note) This paper was based on the author's Ph.D thesis of "Transportation, launching and installation analysis of a truss SPAR" in Newcastle University

coefficient. The mass coefficients are expressed as  $m_{jk}(t)$  and  $m_{jk}$  separately because the spar mass coefficient is time dependent by submerging effects and  $A_{jk}(\infty)$  is constant added mass coefficient.

In calm water condition, the wave exciting force,  $F_j^W(t)$ , is zero, while the event force,  $F_j^E(t)$ , is induced by the sliding motion of the spar in different stages and will be discussed during the following sections.

### 3. Launching Stage

#### - Initial Stage

The initial state of launching is assigned as Initial Stage which is shown in Fig. 1 with zero trim and removed sea-fastenings. The COG (:centre of gravity) of the spar is in line with and directly above the COG of the barge as illustrated. The initial position of the barge's COG is the origin of the assumed local and global coordinate systems.

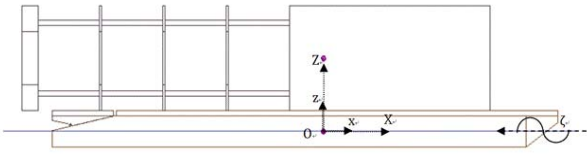


Fig. 1 Initial stage of launching

#### - Stage 1

Stage 1 is defined as the barge is set to a previously established critical trim angle by means of ballast water and the spar is ready to move. In order to determine the critical trim angle, the material on the sliding rail and the frictional resistive force on the rail is needed.

Fig. 2 illustrates the components normal force,  $F_{normal}$ , and sliding force,  $F_{slide}$ , of the weight of a sliding object,  $w_{ob}$ , i.e. the spar on a slope and the frictional force,  $F_{friction}$ . From this concept, variable acceleration, changing velocity, submerged volume effect with hydro drag force and changing barge trim angles with positions of the sliding mass will be discussed and applied to the analysis.

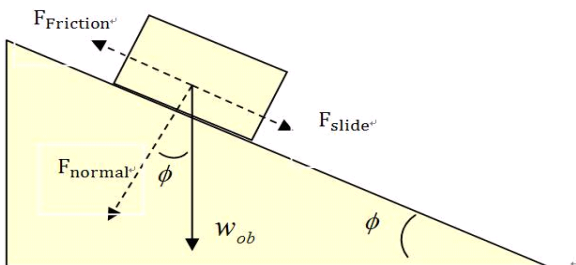


Fig. 2 Force vector diagram in pre-sliding condition

The spar will move naturally at a critical trim angle where the sliding force is greater than the friction force. For the Teflon which has 4% dynamic friction coefficient is usually employed for sliding rail material in industry, the critical trim angle is calculated to be 2.29°

$$F_{slide} > F_{friction} \text{ followed by } \begin{cases} w_{ob} \sin \phi > w_{ob} \sin \phi \\ \tan \phi > 0.04 \\ \phi > 2.29^\circ \end{cases} \quad (2)$$

#### - Stage 2

Although the barge is set to a critical trim angle, the spar structure might not move. This is because the static friction coefficient is greater than dynamic one. To overcome the static friction force, some amount of pushing force should be applied.

The moment of spar hull becomes sliding after overcoming the static frictional force to the time of part of the spar touching water is assigned as Stage 2. The sliding velocity of the spar hull varies with the barge's trim angle which is also changing due to the shifting aft wards of the spar's COG. Increase in the distance between the COG of the spar hull and that of the barge results in larger tilting moment and hence trim angle. The larger the barge's trim angle is, the higher the instantaneous sliding velocity will be.

Using Newton's 2nd law of motion and Eq.(2), the sliding acceleration  $a_1(t)$  of the spar may be written as:

$$a_1(t) = \frac{F_{sliding} - F_{friction}}{m^S(t)} = g \sin \theta(t) - \mu g \cos \theta(t) \quad (3)$$

The sliding velocity of the structure is simply obtained by integration of the acceleration and the distance of travel of the structure is obtained by integration of velocity with respect to time,  $t$ . When the spar is sliding, the change in the relative position of the spar's COG produces a trim moment and hence changes the trim angle,  $\theta_i(t)$ , which may be expressed in the form:

$$\theta_i(t) = \tan^{-1} \left( \frac{m^S(t) \delta(t)}{\rho \nabla GM_L} \right) \quad (4)$$

where  $\delta$  is the distance from the COG of the spar to the COG of the barge,  $\rho$  is water density,  $\nabla$  and  $GM_L$  are the displacement volume and the longitudinal meta-centric height of the barge.

By Newton's 3rd law of motion, the barge will be displaced forwards by the spar movement. From Stage 1, the barge is expected to move until the loss of its moving momentum.

The surge force,  $F_{ds1}$ , induced by the spar movement is equal but opposite to the reaction force on the barge. The sliding acceleration,  $a_1(t)$ , is written as:

$$a_1(t) = \frac{F_{ds1}}{\cos \theta(t) m^S(t)} \quad (5)$$

- Stage 3

Stage 3 is classed as the time when the spar structure is about to touch the water completely, calm water being assumed and part of the spar truss is over-hanging as shown in Fig. 3.



Fig. 3 Schematic view of launching stage 3

The touch length concept is quite important because each member of the spar truss needs a separate calculation for its subsequent submerged volume.

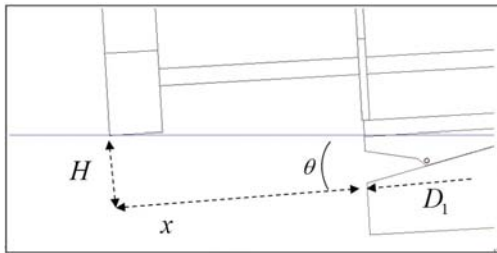


Fig. 4 Touch length diagram

The length of the over-hanged spar shown in Fig.4 is illustrated the touch length,  $S_E$ , and obtained as follows.

$$\tan(\theta) = \frac{H}{S_E} = \frac{H}{D_1 + x} \quad (6)$$

where  $D_1$  is the COG distance of barge.  $H$  is the member's height from the COG of the barge.

Using the sliding acceleration and touching time,  $t_{touch}$ , touch length may be given by

$$S_E = \int_0^{t_{touch}} a_1(t) t dt + S_i \quad (7)$$

where  $S_i$  is the distance from the COG of the barge to the initial position. The touch length of each member changes as the spar's COG.

- Stage 4

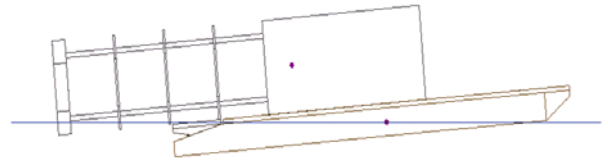


Fig. 5 Schematic view of launching stage 4

Stage 4 is designated as the period from the moment of touching water to the time of the spar's COG is on rocker arm pivot. Several co-related dynamics are observed in this stage. First of all, the spar experiences a buoyancy force with submerged parts as shown in Fig. 5. This results in less weight of the spar on the barge, and also changing the draught and trim angle of the barge.

Apart from this buoyancy, the spar also experiences a hydrodynamic drag force. The drag force induced by water resistance on the spar submerged part will slow down the sliding acceleration and have a change on the trim, etc.

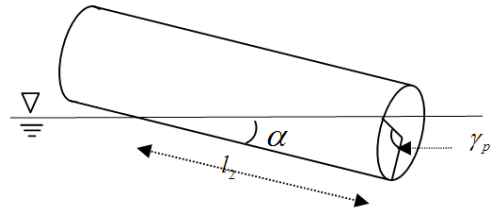


Fig. 6 A typical cylinder entering in water

Since the spar hull has several members of cylinder truss, general formulation of cylindrical type as shown in Fig. 6 can easily be established as following relationships.

$$\begin{aligned} l_2 \tan \alpha &= r(1 - \cos \gamma_p) \\ \cos \gamma_p &= \left(1 - \frac{l_2 \tan \alpha}{r}\right) \end{aligned} \quad (8)$$

where  $l_2, \alpha$  and  $r$  are respectively the submerged length, the inclination angle and the radius.  $\gamma_p$  is the sectional angle from the bottom at the submerged end section. At a distance  $x$  between the end of cylinder and waterline, the sectional angle and the submerged section area  $S_{total}$  are obtained by:

$$\begin{aligned} \gamma : \gamma_p &= x : l_2 \\ S_{total} &= r^2 \theta - r^2 \cos \theta \sin \theta \end{aligned} \quad (9)$$

The volume is calculated by integrating the sectional area from end to the specific length as in the Eq. 10. By integrating sectional area over the submerged length,  $l_2$ , the volume of the submerged part is written in the form:

$$\begin{aligned}
 \nabla &= \int_0^{l_2} r^2 (\theta - \sin\theta \cos\theta) dx & (10) \\
 &= \int_0^{\theta_p} r^2 (\theta - \sin\theta \cos\theta) \frac{l_2}{\theta_p} d\theta \quad (\because dx = \frac{l_2}{\theta_p} d\theta) \\
 &= \frac{l_2}{\theta_p} r^2 \left( \frac{1}{2} \theta_p^2 + \frac{1}{4} \cos 2\theta_p \right)
 \end{aligned}$$

Since the sliding velocity of the spar structure is relatively low, an impact disturbance on the free surface is not expected. Consideration of the drag force due to water resistance is judged to be sufficient. Although the effect of Reynolds number, Keulegan-Carpenter number and wave orbital velocity should be considered to the drag coefficient of each member, representative value can be chosen for the application aspects. The hydrodynamic drag force against the sliding motion may be obtained by:

$$F_{di}^S = \frac{1}{2} \rho C_{Di} A_{Pi} V_R^2 \quad (11)$$

where  $V_R = \frac{1}{dt}(\xi_1^S)$  is relative velocity to the global coordinates.  $A_{Pi}$  and  $C_{Di}$  are projected area and drag coefficient of each member.

The appearance of buoyancy and drag forces on each submerged member will contribute to decelerate the entry rate of the spar. Thus, the modified acceleration,  $a_2$ , may be obtained by

$$m^S a_2 = F_{sliding} - F_{friction} - \sum (F_{bi}^S + F_{di}^S) \quad (12)$$

where  $F_{bi}^S$  is longitudinal force due to the buoyancy of submerged members. The hydrodynamic drag forces,  $F_{di}^S$ , of each member are accounted by its submerged condition. Because of the various member components will not develop their drag at the same time, nor will the rate of development of their individual drag build-up be in-phase with the other components at the same time.

- Stage 5



Fig. 7 Schematic view of launching stage 5

Stage 5 is defined as being the time when the COG of the spar is on the centre of rotation of rocker arm as in Fig. 7. At this moment, the spar is about to rotate. The determination of this moment is needed since the rotational

motion of the spar takes place immediately after that. This is achieved by monitoring the distance from the spar's COG to the centre of rotation and the tilt angle of barge. When the moving distance of the spar's COG to the barge's COG fulfills Eq. 13, it is the time that the spar's COG is just above the centre of rotation.

$$x = l_t - (r^S + h_{rail}^B + h_{tilt}^B) \tan \xi_5^B \quad (13)$$

where  $l_t$  is the distance from the centre of rotation of the rocker arm to the barge's COG,  $r^S$  is the radius of the spar,  $h_{rail}^B$  is the height of rail above deck, and  $h_{tilt}^B$  is the height of the centre of rotation below the deck of the barge.

- Stage 6

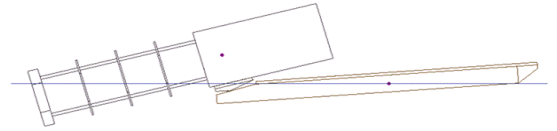


Fig. 8 Schematic view of launching stage 6

Fig. 8 illustrates the Stage 6 that the period of the spar's COG is on the rotating rocker arm after passing the Stage 5 point. If the inertial sliding motion was fast enough to neglect the rotation effect, then the trajectory of the spar could be obtained by calculating directional movement which is induced by gravity acceleration only. In other words, the spar would be projected aft wards without any effect from the rocker arm. However, the motion of the spar in the direction is generally not fast enough for this to happen and the spar is still sliding over and rotating about the pivot point of rocker arm.

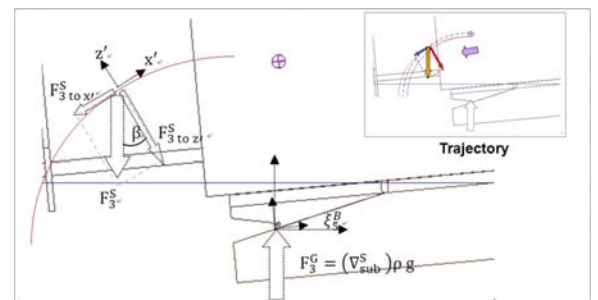


Fig. 9 Trajectory and force vector of the spar's COG

The trajectory of the motion of the spar's COG is divided into rectilinear and rotational motions. Fig. 9 illustrates three different trajectories. The most inner arc is caused only by the rotation of the spar's COG while the most outer arc is obtained from the local x directional velocity and the

incremental time of free drop to the same  $z$  displacement. The trajectory of the spar's COG which is illustrated as the red arc in Fig. 9 starts with the rotational motion and then accounts for the effects of the local  $x$  directional velocity and the free drop.

When the spar's COG passes aft ward beyond the centre of rotation, two force components which are shown in Fig. 9 are observed due to the COG location of spar and the change of submerged volume of the spar. In the surge motion of barge point of view, the inclined location of COG of spar on the rocker arm and inclined buoyancy make surge forces.

The resultant force  $F_1^{BE}$  <sub>weight</sub> can be calculated from the angle of the rocker arm,  $\beta$ , with submerged volume of the spar,  $\nabla_{sub}^S$ , as follows:

$$F_1^{BE}{}_{weight} = (\nabla^S - \nabla_{sub}^S) \rho g \sin(\beta) \cos(\beta) \quad (14)$$

The resultant reaction force of the spar's submerged part  $F_1^{BE}$  <sub>buoy1</sub> can be calculated from the buoyancy of spar's submerged part,  $F_3^G$ , and the trim angle,  $\xi_5^B$ , of the barge as follows:

$$F_1^{BE}{}_{buoy1} = F_3^G \sin(\xi_5^B) = \nabla_{sub}^S \rho g \sin(\xi_5^B) \quad (15)$$

The resultant buoyancy force of the spar's submerged part,  $F_3^{BE} = F_3^G \cos \xi_5^B$ , makes a reaction force,  $F_{3R}^{SE} = F_3^{BE} \cos \beta$ , due to the existence of the spar and the resultant surge force due to the reaction force can be calculated from the angle of the rocker arm,  $\beta$ , and the trim angle,  $\xi_5^B$ , of the barge as follows:

$$F_1^{BE}{}_{buoy2} = \nabla_{sub}^S \rho g \sin(\beta) \cos(\beta) \cos(\xi_5^B) \quad (16)$$

The resultant force on the barge is composed of the spar weight induced force, the reaction force of spar motion and buoyancy force of submerged barge. Those are calculated from Eqs. 14 to 16 and summate as follows:

$$F_1^{BE} = F_1^{BE}{}_{weight} + F_1^{BE}{}_{buoy1} + F_1^{BE}{}_{buoy2} \quad (17)$$

Using the mass of the spar, the buoyancy of the submerged part of the spar, and the distances from the COG of the spar and the centre of buoyancy of the submerged part to the barge's COG, then the heave force and pitch moment on the barge can be easily calculated and should be taken into account on Stage 6 until the spar has finally detached itself from the barge.

Although mechanical friction on the pin of the rocker arm

affects the rotational speed of the arm, it is not considered in the present study. On the other hand, the drag force,  $F_1^{SE}$ , in the global  $X$  direction on the spar due to water resistance is given by with surge velocity,  $\dot{\xi}_{Rl}^S = \dot{\xi}_1^S \cos \xi_5^B$ , of the spar with respect to the global system and the drag moment of the submerged part of the spar structure can be calculated by:

$$F_1^{SE} = \frac{1}{2} \rho C_D A_P (\dot{\xi}_{Rl}^S)^2 \quad (18)$$

$$F_5^{SE} = \sum_{i=1}^n \left[ \frac{1}{2} \rho C_D A_P (r_i \dot{\xi}_{Rl}^S)^2 d_i \right] \quad (19)$$

where  $r_i$  is the distance from the centre of each spar component to the barge's rocker arm centre of rotation and  $d_i$  is the representative local distance from each component of spar to the barge's rocker arm centre of rotation.

- Stage 7

Stage 7 is defined as the instance in time when the rocker arm reaches its mechanically limited angle of rotation as shown in Fig. 10. Nevertheless, this stage and the following stages 8 and 9 will not occur if the spar sliding motion is fast enough to separate itself from the rocker arm before reaching the angle of restriction. This stage can be checked by comparing the limited angle of rotation, with the linear and angular velocities of the spar.

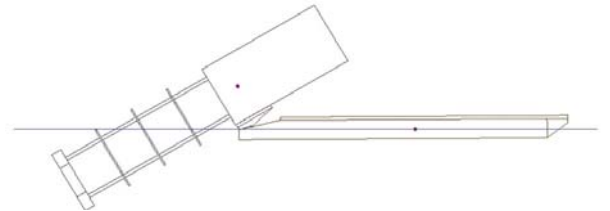


Fig. 10 Schematic view of launching stage 7

- Stage 8

When the rocker arm reaches its maximum angle of rotation, only the sliding motion of the spar is expected on the rocker arm i.e. there are no pitching inertia effects in Stage 8 before separation between the spar and barge. Thus, Stage 8 is the period when the spar structure is sliding downwards on the locked rocker arm until it becomes physically detached from the barge.

- Stage 9

When the spar is about to separate from the barge is assigned as Stage 9. This happens when the spar's COG is just above the aft tip of the rocker arm. The flap on the

trailing edge of the rocker arm is not considered in the present study although it might help to smooth the trajectory of the spar and minimize the tip moment of the rocker arm. When the distance from the spar's COG to the barge's COG fulfills the distance  $x_{sep}$  as shown in Eq. 19, it is the moment in time when the spar's COG reaches the tip of the rocker arm:

$$x_{sep} = l_{end} - (r^S + h_{rail}^B + h_{tilt}^B) \tan \xi_5^B \quad (20)$$

where  $l_{end}$  is the distance of the rocker arm's tip to the barge's COG.

- Stage 10

In Stage 10, the spar and the barge freely float and move separately. The information on the accelerations and velocities of the spar and barge calculated in Stage 9 are used as the initial conditions for the assessment of the separate motions of the spar and barge.

#### 4. Conclusion

The method of a launching analysis is developed based on a time history of the two component bodies with equilibrium conditions

The launching process of the spar hull from the transport barge is divided into ten stages which have different motion and force characteristics.

The drag forces on the submerged parts of the spar structure reduce the sliding acceleration and velocity of the spar. In particular, the effects of changes in buoyancy and drag force due to the progressive submergence of the spar hull have been taken into account by means of a "touch length" idea.

Each stage has a dynamic loading analysis, a motion analysis and a trajectory calculation. Stability and dynamic loadings in the intermediate stages are also examined.

The numerical trajectory model of the spar after the separation have been predicted in order to assess any risk of free floating collision between the spar hull and the barge.

#### Acknowledgement

This research is based on author's Ph.D thesis in New castle University.

#### References

- [1] Noble Denton and Associates Inc. (1984), "Transportation and installation of Offshore Jackets", Technical Policy Boarc, Deck and Modules Section 12.

---

**Received** 27 July 2011

**Revised** 1 September 2011

**Accepted** 2 September 2011